Article

GlialCAM, a CLC-2 Cl^- Channel Subunit, Activates the Slow Gate of CLC Chloride Channels

Elena Jeworutzki,[1,2] Laura Lagostena,[1] Xabier Elorza-Vidal,[3,4] Tania López-Hernández,[3,4,5] Raúl Estévez,[3,4] and Michael Pusch[1,*]

[1]Istituto di Biofisica, Consiglio Nazionale delle Ricerche, 16149 Genoa, Italy; [2]Departments of Anesthesia and Biomedizin, ZLF Lab 408, Universitätsspital Basel, Switzerland; [3]Physiology Section, Department of Physiological Sciences II, School of Medicine, Barcelona, Spain; [4]U-750, Centro de Investigación Biomédica en Red de Enfermedades Raras (CIBERER), ISCIII, Barcelona, Spain; and [5]Department of Molecular Pharmacology and Cell Biology, FMP, Berlin, Germany

ABSTRACT GlialCAM, a glial cell adhesion molecule mutated in megalencephalic leukoencephalopathy with subcortical cysts, targets the CLC-2 Cl^- channel to cell contacts in glia and activates CLC-2 currents in vitro and in vivo. We found that GlialCAM clusters all CLC channels at cell contacts in vitro and thus studied GlialCAM interaction with CLC channels to investigate the mechanism of functional activation. GlialCAM slowed deactivation kinetics of CLC-Ka/barttin channels and increased CLC-0 currents opening the common gate and slowing its deactivation. No functional effect was seen for common gate deficient CLC-0 mutants. Similarly, GlialCAM targets the common gate deficient CLC-2 mutant E211V/H816A to cell contacts, without altering its function. Thus, GlialCAM is able to interact with all CLC channels tested, targeting them to cell junctions and activating them by stabilizing the open configuration of the common gate. These results are important to better understand the physiological role of GlialCAM/CLC-2 interaction.

INTRODUCTION

GlialCAM, formerly called HepaCAM (1), is a cell adhesion molecule primarily expressed in glia (2). *GLIALCAM* is the second disease gene of MLC (3), a rare kind of leukodystrophy characterized by early-onset macrocephaly and myelin vacuolization (4). Interestingly, GlialCAM physically interacts with the gene product of *MLC1*, the first gene found to be mutated in MLC (5). Both proteins colocalize in junctions between astrocytes (3). Recently we found that in astrocytes and oligodendrocytes, GlialCAM is an auxiliary subunit of CLC-2, a rather ubiquitously expressed CLC Cl^- channel (6). In mice, dysfunction of CLC-2 leads to testicular and retinal degeneration and white matter vacuolation (7). The latter phenotype provides a mechanistic link of GlialCAM and CLC-2 functions in glia. The hydrocephalus phenotype and the white matter vacuolation suggest a disturbed water-homeostasis in the brain of MLC patients (8,9). Strong support for a role of CLC-2 in these homeostatic processes is provided by the recent finding that loss of function mutations in CLC-2 lead to white matter edema in humans (9) and by recent studies with *Mlc1* and *Glialcam* knockout mice (10).

GlialCAM affects CLC-2 localization and it strongly modulates its functional properties. With GlialCAM the channel is clustered at cell contacts, especially at astrocyte-astrocyte or astrocyte-oligodendrocyte contacts, but also in heterologous expression systems (6). Furthermore, CLC-2 mediated currents are dramatically activated in heterologous expression systems. The typically slow activation of the inward currents is highly accelerated and deactivation is slowed. In *Xenopus* oocytes GlialCAM greatly amplifies CLC-2 current levels and eliminates current rectification. The effect of GlialCAM on the pH dependence of CLC-2 has led us to speculate that GlialCAM may activate the "common gate" of the channel (6). To obtain insight into the mechanism of channel modulation by GlialCAM, we wanted to test other Cl^- channels as tools since the slow gate mechanism is better understood in them.

A major open question regarding the association of GlialCAM with CLC-2 was if the dramatic activation of CLC-2 currents seen in heterologous expression systems is also found in vivo. This question was answered recently by Hoegg-Beiler et al. (10) who found that in vivo GlialCAM is important for targeting MLC1 and CLC-2 to specialized glial domains in vivo and that in particular in oligodendrocytes GlialCAM activates CLC-2 mediated currents similarly to what is observed in heterologous expression systems (6). Interestingly, no activation of CLC-2 currents was observed in Bergmann glia (10). These data strongly support the idea that not only the GlialCAM mediated targeting of CLC-2 to specialized cell-cell junctions but also the functional activation is physiologically relevant. However, the biophysical mechanisms underlying the activation of CLC-2 by GlialCAM are currently unknown. Therefore discerning the biophysical bases of the interaction between

Submitted April 7, 2014, and accepted for publication July 25, 2014.

*Correspondence: pusch@ge.ibf.cnr.it

Editor: Joseph Mindell.

0006-3495/14/09/1105/12 $2.00

http://dx.doi.org/10.1016/j.bpj.2014.07.040

GlialCAM and the CLC-2 channel is important to better understand the functional and pathological role of GlialCAM.

In our previous work we showed that GlialCAM activates a CLC-2 homolog from Drosophila, whose genome does not contain a GlialCAM homolog, but that it does not alter the currents mediated by CLC-5, a renal Cl^-/H^+ exchanger (6). In this study, we find that GlialCAM interacts in vitro with all CLC channels studied including CLC-0, CLC-1, and CLC-K/Barttin. We exploit these nonphysiological interactions to prove that GlialCAM stabilizes the open conformation of the common gate, providing thus mechanistic insight into the mechanism of activation of CLC-2 by GlialCAM.

MATERIALS AND METHODS

Molecular biology

The channel constructs expressed in oocytes were in the pTLN vector. The Barttin construct in the T3T7 vector and GlialCAM C-terminally tagged with three flag epitopes in the pCSDest vector, as described in earlier studies (6,11). For localization studies, rat CLC-2, human CLC-1, human CLC-Ka, rat CLC-K1, *Torpedo* CLC-0, and human GlialCAM were tagged with a GFP or with flag.

To create the self-cleavable 2A peptide (E2A) Barttin-CLC-K1 construct, we use the following primers:

C term barttin E2A:
5′caccgcatgttagcagacttcctctgccctctccactgccGCCTTGGGTGTCAGGCT CAAAACCCAGCTCCTTTGCCGGG3′
E2A N term CLC-K1: 5′gtctgctaacatgcggtgacgtcgaggagaatcctggccca ATGGAAGAACTCGTGGGACTGCGTGAGGGCTCCTCTGGG3′
Fragments were amplified by PCR and cloned using gateway technology.

Biochemical interaction assays

Biochemical interaction assay were performed using the split-TEV (Tobacco etch virus protease), as described in Jeworutzki et al. (6).

Electrophysiology with oocytes

Oocytes were obtained by surgery and collagenase treatment of ovaries from *Xenopus laevis* frogs. Linearized cDNA was transcribed using the Cell Script AmpliCap™ SP6 High Yield Message Maker Kit (CellScript, Inc., Madison, WI) or the mMessage mMachine kit (Ambion, Life Technologies, Milan, Italy) and the constructs were expressed in oocytes by injection of 5 to 50 ng cRNA according to the expression level of the channel. For GlialCAM, injecting 1.25 ng cRNA was sufficient to achieve the maximal effect (6). To measure a possible increase in the currents by GlialCAM, we adapted the amount of injected channel RNA to maintain relative small currents (<10 μA, to avoid problems of series resistance). Less-diluted cRNA was injected for macro patch experiments to obtain an adequate expression in on-cell patches. For the temperature experiments, the CLC-0 cRNA was reduced when co-injected with GlialCAM together to attain a similar expression level to exclude artifacts because of the observed positive correlation of the offset currents and the amount of expression of CLC-0 (12). Oocytes were kept in a solution containing (in mM) 90 NaCl, 10 HEPES, 2 KCl, 1 $MgCl_2$, 1 $CaCl_2$, pH 7.5, for 2 to 3 days at 18°C. Two electrode voltage-clamp was performed with a Turbotec 03 amplifier (npi, Tamm, npi electronic, Germany) and the custom acquisition program GePulse (freely available at http://users.ge.ibf.cnr.it/pusch/programs-mik.htm). For CLC-1, CLC-2, and CLC-0 the bath solution contained (in mM) 100 NaCl, 5 $MgSO_4$, and 10 HEPES/NaOH pH 7.3. The standard bath solution for CLC-Ka contained (in mM): 112 NaCl, 10 $CaGluconate_2$, 1 $MgSO_4$, and 10 HEPES pH 7.3. Unless otherwise stated, measurements were performed at room temperature (≈20°C). For measurements of the temperature dependence, the temperature of the bath solution was controlled by a custom made temperature control system. For macro patch experiments, the bath solution was (in mM) 100 mM NMDG-Cl, 10 mM HEPES, 2 mM $MgCl_2$, and 1mM EGTA pH 7.3 and kept constantly at 25°C. The pipette (extracellular) solution contained 100 mM NMDG (N-methyl-D-glucamine)-Cl, 10 mM MES and 5 mM $MgCl_2$ (pH 7.3). Boro- or aluminosilicate capillaries (Hilgenberg, Malsfeld, Germany) were coated with Sylgard (Dow Corning Corporation, Midland, MI) and fire-polished. The resistance was adjusted between 0.5 and 2 MΩ, depending on the expression level of CLC-0.

The specificity of the chloride currents of every construct was tested by replacing chloride with iodide (13,14).

Electrophysiology with HEK 293 cells

Fluorescent Human embryonic kidney (HEK) 293 cells, expressing CLC-2-GFP or the double mutant rCLC-2 E211V-H816A-GFP, both in the pFROG vector +/− GlialCAM, were measured with an extracellular solution containing (in mM): 140 NaCl, 2 $MgSO_4$, 2 $CaCl_2$ and 10 HEPES/NaOH pH 7.3 using standard patch clamp technique. Intracellular solution was (in mM) 130 NaCl, 2 $MgSO_4$, 2 EGTA and 10 HEPES/NaOH pH 7.3. Only cells for which currents were reversibly blocked by iodide were used for analysis.

Voltage protocols and data analyses

To dissect hCLC-1 fast and slow gating we used two different protocols. In the first protocol, the overall gating state was monitored using a "tail" pulse to –100 mV after prepulses to variable test voltages (Fig. S1 *C* and *D* in the Supporting Material). In the second protocol, the tail pulse was preceded by a short pulse to 180 mV that fully activated the fast gate without grossly altering the slow gate (15) (Fig. 1 *E* and *F*). This procedure allowed us to determine the open probabilities of the total currents (Fig. S1 *E*) and the slow-gate mediated currents (Fig. 1 *G*) by describing the tail currents with a Boltzmann function.

To estimate the constitutively activated currents of CLC-0 slow gating voltage protocols were applied pulsing from 40 mV, were the fast gate is fully open (16), to –120 mV followed by a tail pulse at 40 mV. From the Boltzmann analysis of the tail currents, we obtained the relative open probability of the slow gate and the constitutive active currents, described by the relative offset.

Deactivation kinetics of CLC-Ka currents in oocytes were analyzed by fitting the decaying current, I(t), at 60 mV with a double exponential function of the following form:

$$I(t) = a_0 + a_f * \exp(-t/\tau_f) + a_s * \exp(-t/\tau_s),$$

where a_0 is the steady state current, a_f the fast decaying component (time constant τ_f), and a_s the slowly decaying component (time constant τ_s).

To study the temperature dependence and the block by 0.2 mM Zn^{2+}, CLC-0 was maximally activated by a long pulse to –120 mV and then the deactivation was followed by pulsing every 2 s to 40 mV while keeping the channel at the resting potential (12).

To compare the currents of the CLC-2 and the double mutant CLC-2 E211V/H816A, oocytes or HEK293 cells were first pulsed to 60 mV to estimate the instantaneous activated current under resting conditions and then activated with a long pulse to –140 mV. The following tail pulse to 60 mV induced a very reproducible current deactivation, which can be best described with a double exponential kinetics. The I_{max} of the tail pulse indirectly reflects the expression level and the ratio I_{ss}/I_{max} the preference of the channel for the open configuration.

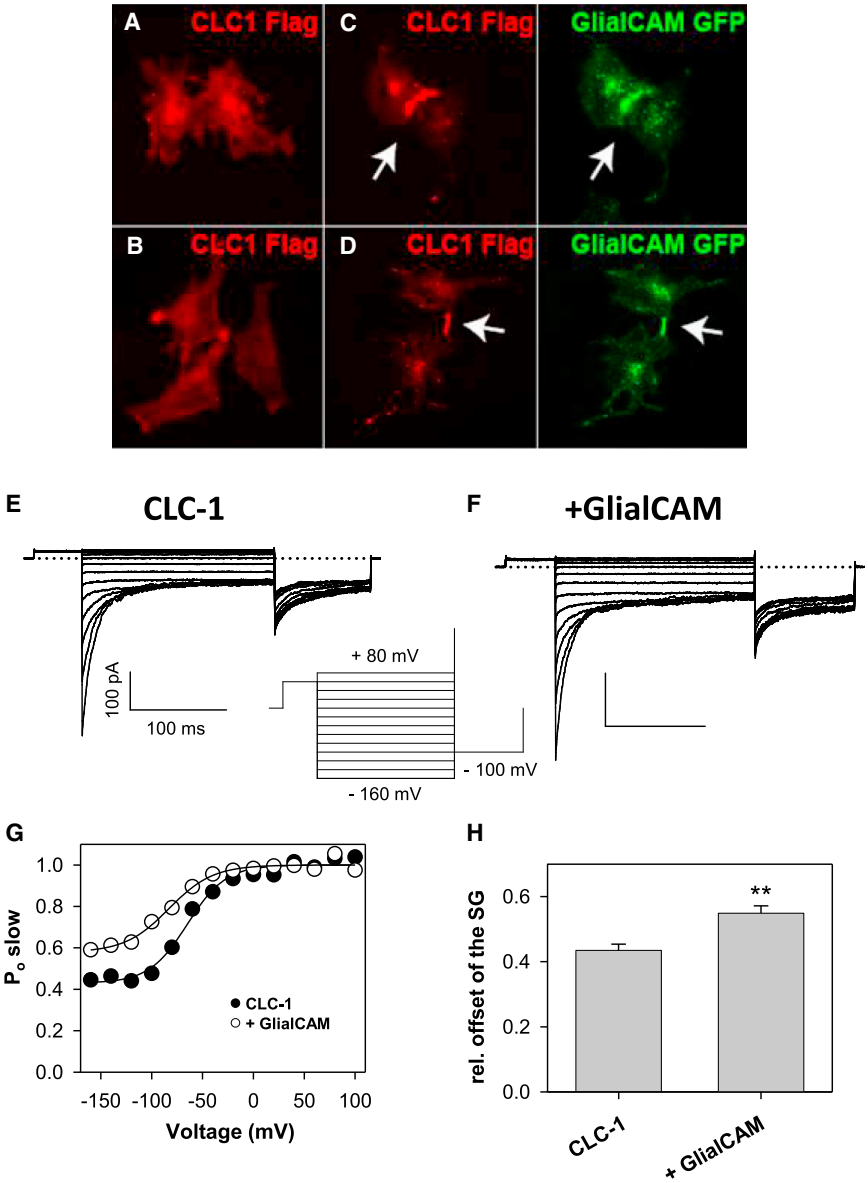

FIGURE 1 Interaction of GlialCAM with CLC-1. (*A–D*) Cellular distribution of CLC-1 in HeLa cells. CLC-1 alone is located uniformly in the plasma membrane and intracellularly (*A*, *B*) whereas GlialCAM changes CLC-1 localization when both proteins are co-transfected to regions of direct contact (*C,* arrow) or to cell-cell contact processes (*D,* arrow). (*E–H*) GlialCAM activates the slow gate of CLC-1 (inset: protocol to determine the open probability of the slow gate; see Methods). (*E*, *F*) typical currents from a patch from oocytes expressing CLC-1 alone (*E*) or CLC-1 with GlialCAM (*F*). (*G*) Initial (I_o) tail currents from the patches shown were described with a Boltzmann function (plus offset) and the open probabilities of the example patches are plotted against voltage. The relative offset of the slow gate (*H*) is significantly larger with GlialCAM (**p $<$ 0.01, Student's *t*-test, values are mean $\pm$SE). Voltages of half-maximal activation were not significantly different (data not shown). To see this figure in color, go online.

Raw data were analyzed using a custom analysis program (Ana; freely available at http://users.ge.ibf.cnr.it/pusch/programs-mik.htm), Excel (Microsoft Corp., Redmond, WA), and Sigma Plot (Systat Software, Inc., San Jose, CA). To indicate statistical significance we depict mean values $\pm$ SE and annotate p-values of Student's *t*-test or of Bonferroni's multiple comparison test.

RESULTS

GlialCAM interacts with CLC-1 and leads to CLC-1 clustering in cell-cell contacts

In our previous work we showed that GlialCAM strongly clusters CLC-2 at cell-cell contacts (6). We tested whether GlialCAM promotes a similar clustering of the muscle CLC-1 channel. CLC-1 expressed alone in HeLa cells is detected mostly all over the cell, especially around the nucleus and on the cell surface (Fig. 1 *A* and *B*). When co-expressing GlialCAM, CLC-1 changes its localization pattern extensively to the places of cells contacts largely overlapping with the localization of GlialCAM (Fig. 1 *C* and *D*; marked by arrows). A similar clustering of CLC-1 in cell-cell contacts upon co-expression with GlialCAM was seen in HEK 293 cells (data not shown). The biochemical interaction was confirmed by Split TEV assay (Fig. S1 *A* and *B*).

GlialCAM slightly increases the residual open probability of CLC-1 channels in oocytes

To determine whether GlialCAM has a functional effect on CLC-1 mediated currents, we co-expressed GlialCAM and CLC-1 in *Xenopus* oocytes and performed inside-out patch clamp recordings that allow a high-resolution quantitative separation of fast and slow gating kinetics using two different pulse protocols (15) (Figs. 1 *E* and *F*; and S1 *C* and *D*).

The gating parameters of the fast gate are very similar for CLC-1 and CLC-1/GlialCAM (Fig. S1 *E* and *F*). In contrast, for the slow gate, the residual activation at negative voltages is significantly increased by GlialCAM co-expression (Fig. 1 *G* and *H*). Thus, localization studies, biochemical data, and functional expression demonstrate that CLC-1 and GlialCAM interact. However, the functional effect on CLC-1 is rather small compared with the dramatic effects seen for CLC-2 (6).

GlialCAM slows deactivation of the CLC-Ka/Barttin kidney Cl^- channel

CLC-Ks belong to the CLC-1-like branch of plasma membrane localized CLC Cl^- channels (17). They share ~ 50% sequence identity with CLC-0, CLC-1, and CLC-2. Estévez et al. (18) showed that Barttin is a β-subunit of human CLC-K channels necessary to target the channels to the plasma membrane. Co-expression of CLC-Ka with GlialCAM without Barttin did not induce any currents different from control oocytes (Fig. 2 *B*). Interestingly, the co-expression of all three proteins, CLC-Ka, Barttin, and GlialCAM induces currents that are similar to CLC-Ka/Barttin, but which exhibit markedly slower deactivation kinetics at 60 mV (Fig. 2 *C*, *D*, and *G*). Maximal (Fig. 2 *E*) or steady-state currents (Fig. 2 *F*) at 60 mV were not different. This modulation of the gating kinetics demonstrates that CLC-Ka is able to interact simultaneously with Barttin and with GlialCAM suggesting that the binding region is different for both interaction partners.

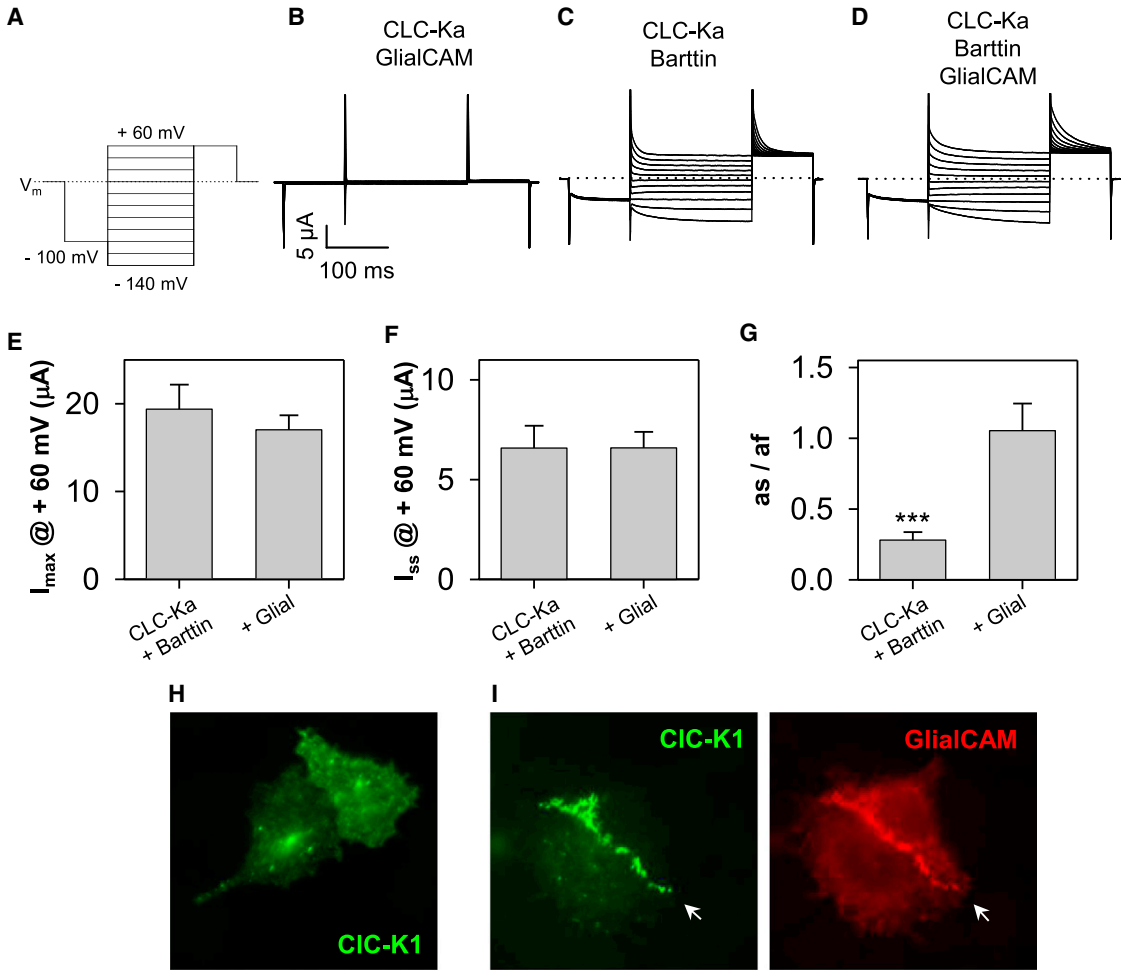

FIGURE 2 hCLC-Ka/Barttin mediated currents are modulated by GlialCAM. (*A*) Pulse protocol. (*B–D*) Typical currents from oocytes injected with CLC-Ka and GlialCAM (*B*), CLC-Ka and Barttin (*C*), or CLC-Ka, Barttin, and GlialCAM (*D*). Amount of cRNA for each construct was kept constant in the different co-injections. In (*C*) and (*D*) same scale bars as in (*B*). From the tail current after the –140 mV prepulse, the initial current (I_{max}), shown in (*E*) and the steady state current (I_{ss}), shown in (*F*) were determined. A double exponential fit to this tail current yielded time constants and coefficients of the two exponential components (see Methods). Fast and slow time constants were for CLC-Ka/Barttin 43 ± 11 ms and 6.8 ± 1 ms, for CLC-Ka/Barttin/GlialCAM 36 ± 1 ms and 8.7 ± 0.3 ms, respectively (n = 10), i.e., not significantly different. (*G*) Ratio of slow (as) and fast coefficient (af) of the double exponential: the weight of the slow component is significantly increased by GlialCAM. (***p < 0.001, Student's *t*-test), values are mean ± SE. (*H–I*) Cellular distribution of CLC-K1 in HeLa cells. Barttin-CLC-K1 alone is located uniformly in the plasma membrane and intracellularly (*H*) whereas GlialCAM leads to CLC-K1/barttin localization in regions of cell-cell contacts (*I,* arrow). To see this figure in color, go online.

To test if GlialCAM is able to redirect CLC-K channels to cell contacts, initially CLC-Ka was co-transfected in HEK cells either with only Barttin or GlialCAM or with both subunits. Without GlialCAM, no clustering could be observed (n = 5 transfections, data not shown). In co-transfections with GlialCAM (with and without Barttin), a few cells could be observed that showed clustering at cell-cell contacts (Fig. S2). This suggests that in principle GlialCAM is able to direct CLC-K channels to cell contacts, even in the absence of Barttin, however with relatively low efficiency. In particular, for the co-transfections of CLC-Ka, Barttin, and GlialCAM, the low efficiency of clustering could be attributable to a low probability to have couples of adjacent cells that are both triple-transfected. To overcome the latter difficulty, we created a Barttin-CLC-K1 construct in which the two cDNAs were linked by a self-cleavable 2A peptide. The 2A peptide mediates a co-translational cleavage producing multiple proteins from a poly-protein encoded by a single open reading frame (19). HeLa cells were transfected with the construct alone (Fig. 2 *H*) or together with GlialCAM (Fig. 2 *I*). In the co-transfected cells GlialCAM and CLC-K1 co-localize clearly at the cell-cell contact.

GlialCAM does not interact with the CLC-5 transporter

To determine if GlialCAM clustering is specific to CLC channels, we tested whether GlialCAM promotes clustering of the CLC-5 exchanger. CLC-5 expressed alone in HeLa cells is detected mostly all over the cell cytoplasm (Fig. 3 *A*). When co-expressing GlialCAM, CLC-5 does not change its cellular localization, with no clear co localization at cell-cell contacts (Fig. 3 *B*). These data confirm our previous work, reporting that GlialCAM does not alter CLC-5 mediated currents (6). Thus GlialCAM is not able to interact functionally or biochemically with the CLC-5 transporter.

GlialCAM opens the slow gate of CLC-0

CLC-0 is a well-studied model channel that allows a relatively easy distinction of fast and slow gating mechanisms (12,16,20–29). To study if GlialCAM has some functional effect on CLC-0, we used two electrode voltage clamp and macro patch recordings of *Xenopus* oocytes. The fast gate transients of CLC-0 +/− GlialCAM did not show any differences (Fig. S3).

The slow gate was studied by applying long voltage pulses going from positive to negative voltages followed by a tail pulse to 40 mV (Fig. 4 *A*). The slow gate starts to increase its open probability at voltages more negative than −60 mV that becomes visible at the positive tail pulse, where the fast gate opens maximally (12) (Fig. 4 *B* and *C*). CLC-0 co-expressed with GlialCAM exhibits a large constitutive conductance at positive voltages and can only be marginally further activated by hyperpolarization (Fig. 4 *B*, *D*, and *E*).

Comparing these tail currents of CLC-0 +/− GlialCAM (Fig. 4 *B* and *C*) shows that the residual open probability is largely increased when GlialCAM is co-expressed (Fig. 4 *F*). Also in macro patch on-cell experiments the relative offset of the slow gate was increased from ~ 0.2 without GlialCAM to a value of ~ 0.6 when GlialCAM was co-expressed (Fig. S4).

When CLC-0-GFP was co-transfected with GlialCAM in HEK293 cells, clusters at cell contacts were observed in 19 cell pairs of eight plated dishes (Fig. 4 *G*), demonstrating physical interaction between the two proteins. To test if the macroscopic functional effects on the slow gate represent the properties of a pure population of GlialCAM/CLC-0 complexes, or a mixture of such complexes with GlialCAM free CLC-0 dimers, we performed a titration experiment in which we compared the properties of oocytes injected with increasing amounts of GlialCAM RNA, concentrating on the relative offset of the slow gate as a functional readout (Fig. 4 *H*). In the experiment shown in Fig. 4 *H*, the half-maximal effect of GlialCAM is seen at an amount of 0.25 ng RNA per oocyte and saturation at 1 ng (Fig. 4 *H*). Thus, most likely, at the standard amount used (2.5 ng) GlialCAM/CLC-0 complexes are the predominant species. This conclusion is qualitatively in agreement with the observation of a large percentage of clustering seen in HEK cells. Nevertheless, from these experiments no quantitative conclusion of interaction strength can be drawn.

Taken together, GlialCAM is able to interact with CLC-0, clustering the channel at cell contacts and favoring the open conformation of the slow gate represented by a large constitutive open probability, which is

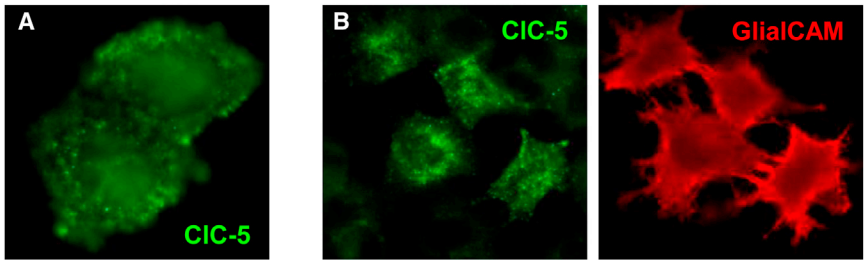

FIGURE 3 Co-expression of GlialCAM with CLC-5 in HeLa cells. (*A*). Cellular distribution of CLC-5 alone. (*B*). GlialCAM does not modify CLC-5 localization when both proteins are co-transfected. To see this figure in color, go online.

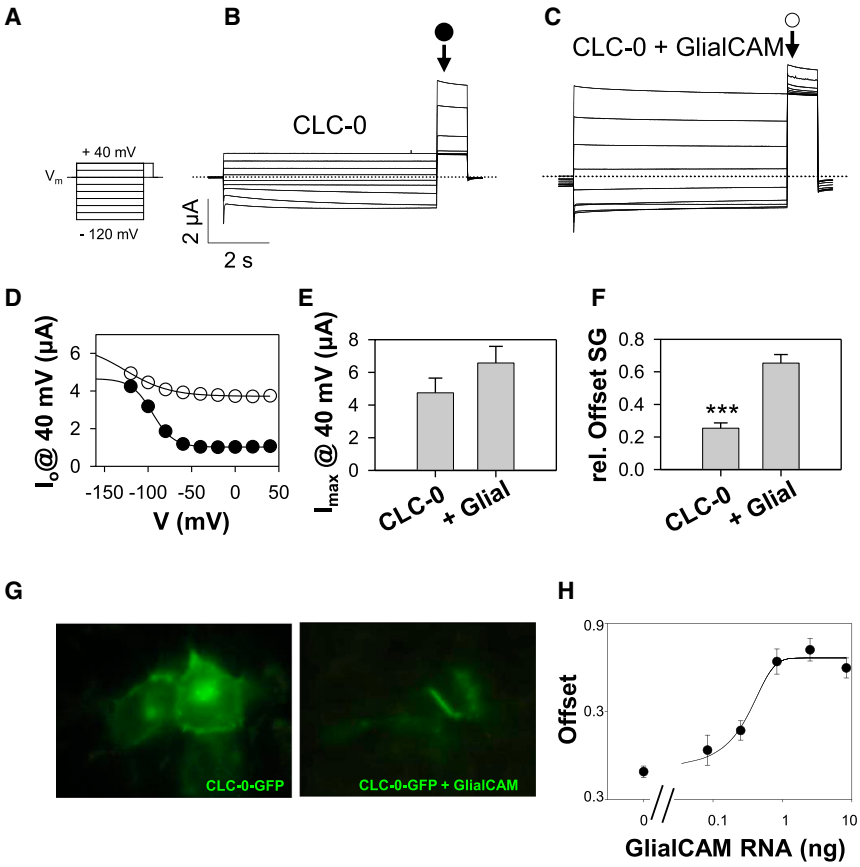

FIGURE 4 GlialCAM activates the slow gate of CLC-0. (*A*) Pulse protocol used to assay the slow gate. (*B*, *C*) Typical current traces obtained with this protocol for CLC-0 (*B*) and CLC-0/GlialCAM (*C*). (*D*) Example tail currents from the current traces shown in (*B*) and (*C*) plotted as a function of the prepulse voltage and fitted with a Boltzmann function with offset (lines). (*E*) Maximal current at 40 mV obtained from the Boltzmann analysis (*F*) Relative offset obtained from the Boltzmann analysis (***p $<$ 0.001, Student's *t*-test). *(G)* GlialCAM-induced clustering of CLC-0-GFP in HEK293 cells. *(H)* Dose-response of increasing concentration of GlialCAM on relative offset of the slow gate. Amount of CLC-0 RNA was 0.25 ng/oocyte. Data were fitted by a "Boltzmann equation" resulting in a half maximal amount of 0.25 ng/oocyte GlialCAM RNA (qualitatively similar results were seen in a total of three batches of oocytes). To see this figure in color, go online.

similar, but much more dramatic, to what we observed for CLC-1.

Slow gate deactivation of CLC-0 / GlialCAM channels remains temperature sensitive

Slow gating of CLC-0, and in particular its deactivation kinetics, is highly temperature sensitive with a Q10 of ~ 40 (12). To test if GlialCAM affects the temperature sensitivity we measured the deactivation kinetics of the slow gate (12). After maximally activating the slow gate by repetitive hyperpolarization, the activation status of the slow gate was monitored by short pulses to 40 mV, keeping the oocytes at the resting voltage (Fig. 5 *A*; example traces at 33°C). The deactivation kinetics were described by a single exponential function, from which we obtain the time constant, τ, of the deactivation (Fig. 5 *B*) and the percentage of deactivation (Fig. 5 *C*). The time constant is significantly

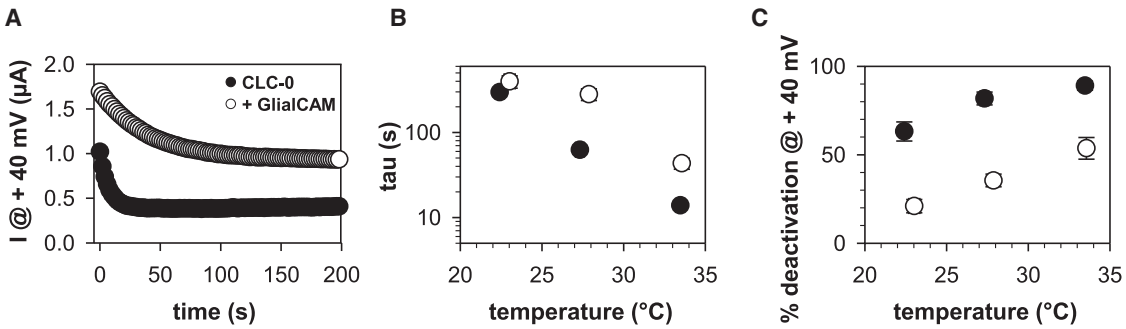

FIGURE 5 Temperature sensitivity of the deactivation kinetics of the slow gate. (*A*) Current decay at resting conditions, monitored by brief pulses every 2 s to 40 mV, after a long hyperpolarizing pulse (T = 33°C for this example). (*B*, *C*) Current deactivation was described by a single exponential function yielding the time constant (*B*) and the percentage of deactivation (*C*) as a function of temperature. Due to the very slow deactivation of CLC-0/GlialCAM at lower temperatures, it was not possible to obtain a reliable value for the time constant (n = 4 to 7 for each temperature from a total of 5 to 10 different oocyte batches; error bars represent SE).

larger and the percentage of deactivation significantly smaller for CLC-0/GlialCAM compared with CLC-0 expressed alone. However, the temperature dependence is comparable between CLC-0 and CLC-0/GlialCAM. Thus, even though the open configuration of the slow gate in the CLC-0/GlialCAM complex is stabilized dramatically, it retains the characteristic temperature dependence of the slow gate.

CLC-0's sensitivity to Zn^{2+} inhibition is largely reduced

CLC-0 inactivation was shown to be greatly facilitated by extracellular Zn^{2+} (26). We found that the CLC-0/GlialCAM complex exhibits a very weak block by 0.2 mM Zn^{2+} (Fig. 6 *A*). The percentage of block is more than 70% reduced for CLC-0/GlialCAM expressing oocytes compared with CLC-0 alone (Fig. 6 *B*).

CLC-0 open phenotype gating mutants do not exhibit further activation by GlialCAM

The maximal current level of CLC-0 at 60 mV that is achieved by saturating activation of the slow gate by repetitive hyperpolarization is roughly doubled by co-expression with GlialCAM (Fig. 7 *C*, *D*, and *I*; $p < 0.05$). We wanted to test if this current increase is additionally caused by a larger number of channels present in the plasma membrane (with GlialCAM), or if it only reflects a submaximal activation of the slow gate by hyperpolarization (without GlialCAM). To this end we employed gating mutants of CLC-0 that are unlikely to disturb the biochemical interaction between the two proteins, as being shown for CLC-2 mutants that abolish the slow gate (see below; Fig. 8). Mutant C212S locks the slow gate in the activated state (26). Further activated is the double mutant C212S/E166C where the neutralization of the gating glutamate constitutively activates the fast gate and the slow gate (28,30). To study the constitutive and maximally activatable current levels (for WT CLC-0) we first applied short pulses to 60 mV without previous activation of the slow gate by hyperpolarization, followed by a pulse to −160 mV for 200 ms. These pulses were applied repeatedly until there was no further current increase. Fig. 7 *C*, *E,* and *G* present typical current traces of CLC-0 and the two mutants C212S and E166C/C212S. CLC-0 exhibits around 50% of current activation by repetitive hyperpolarization (Fig. 7 *C* and *J*). When co-expressed with GlialCAM no significant further current increase could be induced by negative voltages (Fig. 7 *D* and *J*). As expected, for mutants C212S and C212S/E166C, no activation by hyperpolarization is seen without or with GlialCAM (Fig. 7 *E–H* and *J*).

More interestingly, the co-expression with GlialCAM did not increase the maximal current level for these two mutants, suggesting that GlialCAM does not increase the number of channels in the plasma membrane (Fig. 7 *I*).

GlialCAM clusters CLC-2 'open-phenotype-mutant' E211V/H816A but currents are not significantly changed

The double mutant E211V/H816A of CLC-2 where the gating glutamate and a C-terminal histidine (31) are mutated, results in a constitutive activation of the slow gate in CLC-2 (32). Indeed, expressing this construct in HEK293 cells or oocytes resulted in constitutively activated channels as described (32) (Fig. 8 *A* and *B*). Co-expression of this double-gating mutant with GlialCAM (Fig. 8 *C* and *D*) leads to a slight increase of currents in oocytes (Fig. 8 *D*) but not in HEK cells (data not shown).

Importantly, GlialCAM has no effect on the biophysical properties of the double mutant (Fig. 8 *E*). In HEK 293 cells, co-expression of the E211V/H816A mutant with GlialCAM leads to the clustering of the CLC-2 mutant in cell contacts, demonstrating that the mutant does not interfere with the biochemical interaction (Fig. 8 *C*).

DISCUSSION

Combining the present and our previous study (6) shows that GlialCAM is able to interact with all CLC channels tested so far, i.e., mammalian CLC-1, CLC-2, and CLC-Ka, *Drosophila* CLC-2 (dmCLC-2), and *Torpedo* CLC-0 (see Table 1) for summary). The interaction of GlialCAM with

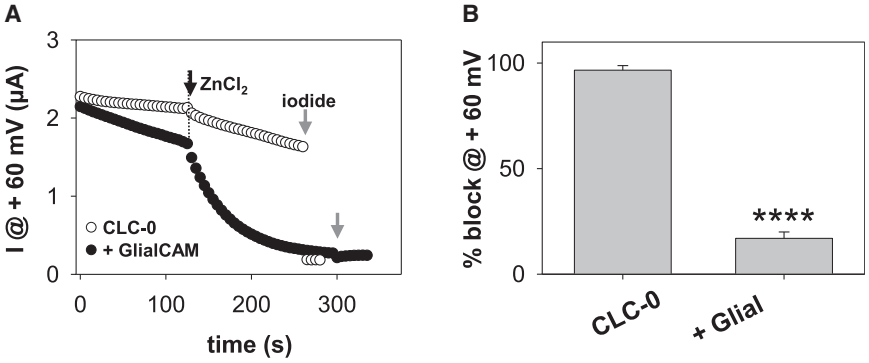

FIGURE 6 GlialCAM reduces Zn^{2+} sensitivity of CLC-0. (*A*) CLC-0 (*closed circles*) and CLC-0/GlialCAM (*open circles*) were activated by a long hyperpolarizing pulse and then deactivation at the resting voltage was monitored by brief pulses to 60 mV. 0.2 mM Zn^{2+} was applied at the indicated time point. At the end of the experiment, Cl^- was replaced by iodide (*gray arrow*) to estimate leak currents. (*B*) Percentage of block by 0.2 mM Zn^{2+} of CLC-0 ± GlialCAM ($n \geq 4$ different oocytes ± SE each; ****$p < 0.0001$, Student's *t*-test).

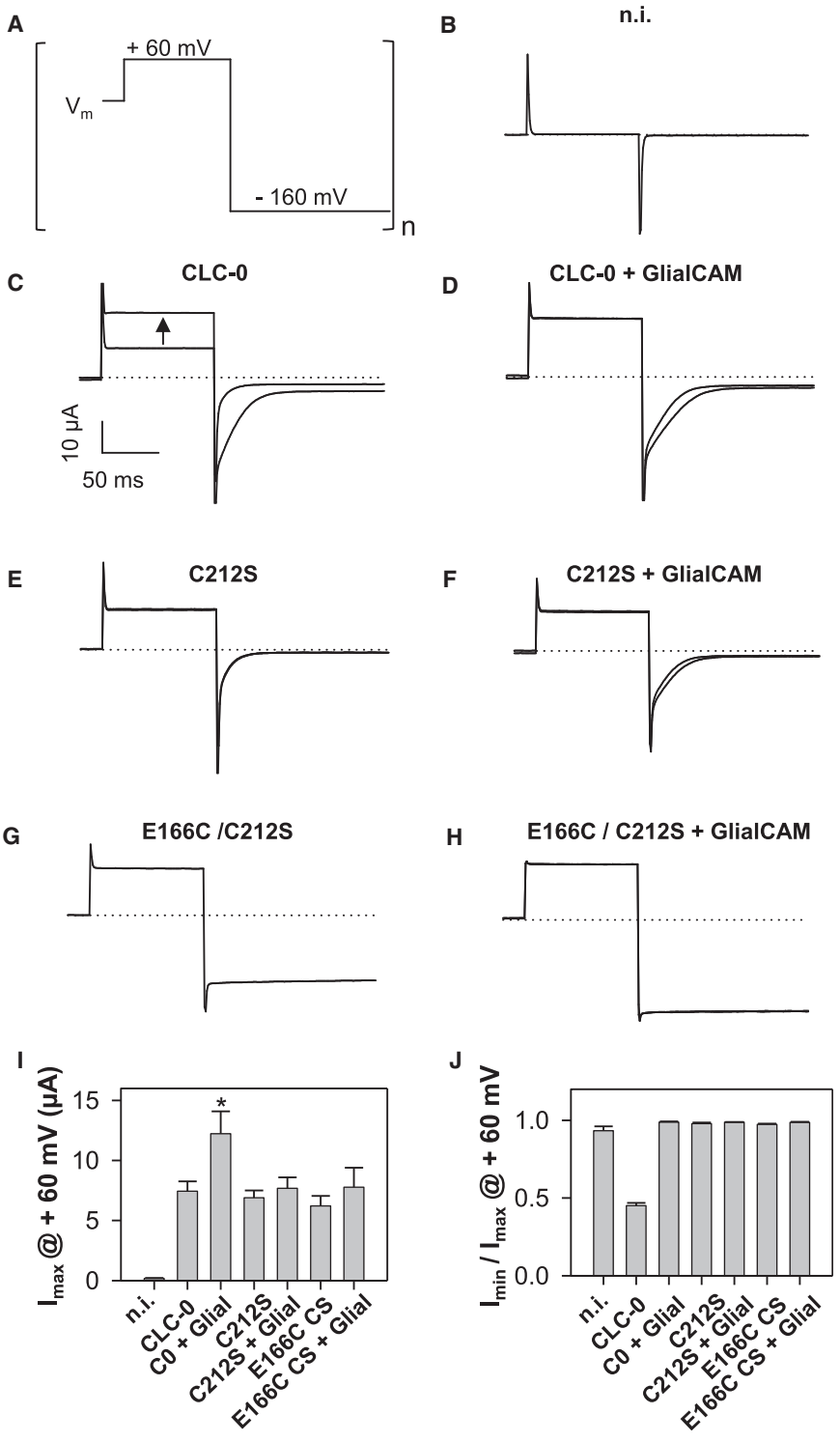

FIGURE 7 Effect of GlialCAM on currents of CLC-0 gating mutants. (*A*) Voltage pulse that was repetitively applied to maximally activate the slow gate. (*B*) Currents from an uninjected control oocyte. (*C*) Example traces from a CLC-0 expressing oocyte before and after maximal activation of the slow gate. (*D–H*) Similar examples for CLC-0+GlialCAM (*D*), C212S (*E*), C212S+GlialCAM (*F*), E166C/C212S (*G*), and E166C/C212S+GlialCAM (*H*). (*I*) Maximal currents of the indicated constructs for one batch of oocytes, similar results were seen in four batches (*$p < 0.05$, Bonferroni's test). (*J*) I_{min}/I_{max} for the indicated constructs, representing the ratio of the currents at 60 mV before and after repetitive application of the pulse shown in (*A*) ($n > 6$ oocytes for each construct).

CLC-1 and CLC-K is probably of no physiological relevance because these two channels are not expressed in glia. Even though it cannot be excluded that related proteins could play similar roles in muscle, kidney, or inner ear, the sites of expression of CLC-1 and CLC-K channels, the closest homolog of GlialCAM, HepaCAM2, does not interact with CLC-2 (6).

In all cases tested (CLC-1, CLC-2, CLC-K, *Torpedo* CLC-0, and dmCLC-2) the interaction results in the clustering of the channels at cell-cell contacts, after the localization of GlialCAM. This and the fact that most of the disease inducing mutants of GlialCAM exhibit a disturbed clustering phenotype strongly suggests that the precise localization of the interaction partners is physiologically very important (3,6).

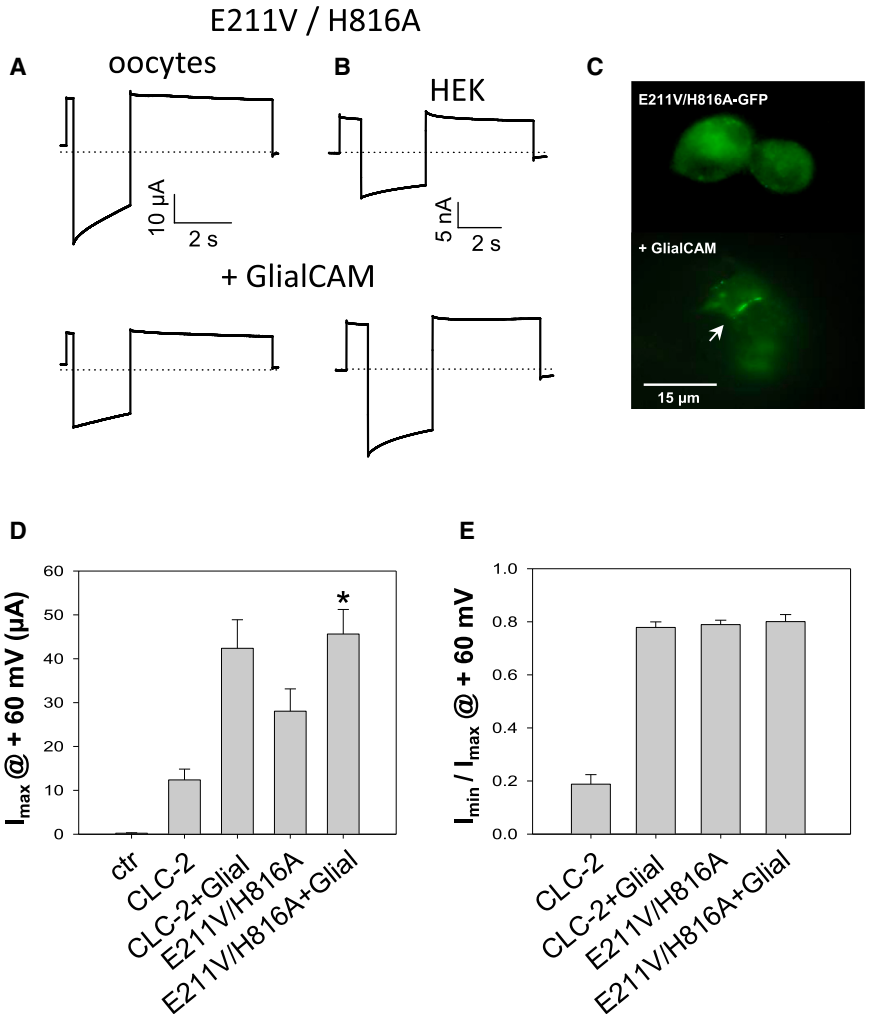

FIGURE 8 CLC-2 double gating mutant E211V/H816A expressed in HEK cells and oocytes. (*A*, *B*) Typical current traces obtained by a voltage pulse to 60/–120/60 mV in oocytes (*A*) and HEK293 cells (*B*) for the double mutant without (*top*) or with (*bottom*) GlialCAM. (*C*) Fluorescence of HEK cells expressing the E211V/H816A mutant C-terminally fused to GFP without (*top*) or with (*bottom*) GlialCAM. (*D*) I_{max} at 60 mV was slightly increased for E211VH816A when co-expressing GlialCAM in oocytes (*$p < 0.05$, Bonferroni's test). Note, that in patch clamp experiments of HEK cells GlialCAM does not increase the currents of the double mutant. (*E*) In contrast to CLC-2 co-expressing the double gating mutant with GlialCAM does not alter its current characteristics as assayed by the ratio of steady state currents and I_{max} at 60 mV ($n \geq 6$ cells from two different transfections/injections; error represents SEM). To see this figure in color, go online.

On the other hand, GlialCAM does not interact with the more distantly related CLC-5 transporter (this work and (6)). Thus, the interaction with GlialCAM is less specific, in comparison with the highly specific interaction of Barttin with CLC-K channels (18) and of Ostm1 with the intracellularly localized CLC-7 (33,34). The auxiliary subunit Barttin is essential for efficient targeting and trafficking of the CLC-K channels to the plasma membrane (18,35). Similarly, it was shown also for GlialCAM that it stabilizes MLC1 (36), the first identified GlialCAM binding partner (3). Our previous observation that CLC-2 currents are largely increased when GlialCAM is co-expressed (especially in oocytes) (6) might support the idea that GlialCAM stabilizes also the CLC-2 protein in the plasma membrane (by either increasing its insertion rate or by decreasing the retrieval rate). Alternatively, the large current increase could reflect a modulation of the gating of the channel, resulting in an increased open probability.

In the *Torpedo* CLC-0 channel, the so-called fast gate or protopore gate can close individual protopores and is fundamentally dependent on the so-called gating glutamate (E166 in CLC-0) (27,30,37). Additionally, both pores can be simultaneously switched off by a mechanism called slow gate (38), because it acts in the seconds-to-minutes range, whereas the fast gate opens and closes in the milliseconds time range. The two gates of CLC-0 are not independent. For example the CLC-0 mutants E166A or E166D not only affect the fast gate but they also lock the slow gate in an open configuration (28). Slow gating depends on pore occupancy because low external (16) and internal (39) [Cl^-] favor slow gate closure. However, the impressive temperature sensitivity of CLC-0 slow gating, with a Q10 of the deactivation kinetics at positive voltages around 40, points to a complex rearrangement of the channel (12). Also block by Zn^{2+} is highly temperature sensitive and reflects a closure of the slow gate (20). The CLC-0 mutant C212S eliminates Zn^{2+} block and also locks the slow gate in an open conformation (26).

A slow or common gate was also identified in CLC-1 and CLC-2, which has however different quantitative properties in these channels (32,40–48). In particular, fast and slow gating have different voltage dependencies (40,49) and slow gating is less temperature sensitive (47,50) in CLC-1 and CLC-2. Importantly, the key mutations of the gating

TABLE 1 Effect of GlialCAM on biophysical properties of different CLC channels and transporters

	Clustering strength*	Increase of I_{max} at positive V (in oocytes)	Activation of slow gate†	Slowed kinetics of deactivation at positive voltages‡
CLC-2	+++	15-fold	+++	+++
CLC-2E221V/H816A	+++	No	-	n.a.
CLC-1	+++	No	+	n.a.
CLC-0	++	3.9-fold	+++	+++
CLC-Ka	+	No	n.a.	n.a.
CLC-Ka+Barttin	+	No	n.a.	+
Barttin-2A-CLC-K1	++	No	n.a.	+
CLC-5	-	No	n.a.	n.a.

*The strength of interaction is qualitatively indicated by the number of + signs reflecting the number of clusters found per number of transfected dishes: CLC-2: 9/3; $CLC\text{-}2_{E221V/H816A}$: 21/7; CLC-1: 28/8; CLC-0: 19/8; CLC-Ka: 13/13; CLC-Ka+Barttin: 9/13; Barttin-2A-CLC-K1: 9/4; CLC-5: 0/3. †the number of + signs qualitatively indicates that the slow gate is strongly activated in CLC-0 and CLC-2 but only slightly in CLC-1; ‡the number of + signs qualitatively indicates that the deactivation kinetics is strongly affected in CLC-2 and CLC-0 and less in CLC-Ka. n.a.: not applicable.

glutamate and the cysteine corresponding to C212 of CLC-0 drastically affect slow gating also in CLC-1 and CLC-2 (15,47). Interestingly, slow gating is dependent on the cytosolic C terminus of the channels that contains two so-called CBS domains (31,32,48,51,52), and that have been proposed to undergo a large conformational change during slow gating transitions (53,54).

Even less understood are the gating mechanisms of CLC-K channels, which are associated with the small Barttin subunit. Even though the "gating glutamate" is replaced by a valine in CLC-K channels, they undergo time- and voltage-dependent relaxations, in particular when expressed in *Xenopus* oocytes (11,18). At the single-channel level CLC-K channels exhibit a double-barreled appearance (55). However, the relationship of the mechanisms underlying CLC-K gating with those of CLC-0, CLC-1, and CLC-2 is still not clear.

Here we exploited the interaction of GlialCAM with other CLC channels to investigate the biophysical mechanisms underlying the strong activation of CLC-2 mediated currents by GlialCAM.

Although functional effects on CLC-1 were rather subtle, we could verify a dramatic activation of CLC-0, caused by an increase of the open probability of the slow (common) gate of the channel. Several lines of evidence, including two-electrode voltage clamp measurements, patch-clamp recordings, investigation of temperature dependence and Zn^{2+} block, and the investigation of slow gate deficient mutants, point to the same conclusion: in the protein complex CLC-0/GlialCAM the open conformation of the slow gate is significantly stabilized compared with CLC-0 alone. In contrast, the number of channels expressed in the plasma membrane is not significantly increased by GlialCAM. It is thus natural to make the same conclusion regarding the functional effect of GlialCAM on CLC-2, even though the slow gate is less well defined for CLC-2. Strong evidence in support for the conclusion that GlialCAM activates the common gate also for CLC-2 was obtained by investigation of the interaction of GlialCAM with the CLC-2 mutant E211V/H816A in which the common gate is locked open (32): although GlialCAM targets the mutant to cell-contacts just as WT, it has almost no effect on the current magnitude in oocytes or in HEK cells.

Thus, taken together, we can conclude that, in general, GlialCAM interaction results mainly in a stabilization of the open configuration of the common gate of CLC-channels. Thus, the future identification of the interaction sites of CLC channels with GlialCAM might be helpful to gain insight into the mechanisms underlying the slow gate, which is still poorly understood.

A somewhat unexpected result is that GlialCAM is able to interact with CLC-K/Barttin channels, although it cannot substitute for Barttin. The interaction of CLC-Ka/Barttin with GlialCAM results in a slowed deactivation of currents at positive voltages. This suggests that the gating kinetics of CLC-K channels reflect relaxations of the common gate in agreement with other studies (55,56). In addition, this result shows that CLC-Ka, Barttin, and GlialCAM are able to form a heteromeric complex (of unknown stoichiometry) and thus that Barttin (a 2 trans membrane domain (TMD) protein) and GlialCAM (a 1 TMD protein) interaction sites with CLC-Ka do not significantly overlap. It will be interesting to dissect the interaction sites of these three proteins.

The properties of CLC-2 are highly dependent on the expression system (39,46,49,57,58), and also the increase of currents caused by GlialCAM is less pronounced in HEK cells than in *Xenopus* oocytes (6). These differences might be caused by various mechanisms, including different posttranslational modification (e.g., glycosylation (59)), different modes of interaction involving cytosolic domains of the proteins (e.g., the CLC-2 N-terminus (13,46,57)) or interactions with the cytoskeleton (60). Recently (10) the functional network of MLC1, GlialCAM, and CLC-2 and its role in leukodystrophy was investigated in vivo, by studying mice that lack MLC1, CLC-2, or GlialCAM. As expected, loss of GlialCAM changes the localization and abundance of CLC-2 and MLC1 in glia. Interestingly, activation of CLC-2 currents by GlialCAM was clearly observed in oligodendrocytes but not in Bergmann glia (10). This in vivo study positively answers the question whether the functional effect of GlialCAM on CLC-2 occurs also in a physiological setting, even though the selective activation in oligodendrocytes remains mysterious.

In this respect, it is important to investigate the biophysical mechanisms underlying the activation of CLC-2 mediated currents by GlialCAM. In this study, using as a tool the interaction of GlialCAM with other CLC channels, we

obtained significant insight into these mechanisms. We showed that GlialCAM is able to interact with all tested CLC channels (CLC-0, CLC-1, CLC-2, dmCLC-2, and CLC-K/Barttin) even though, except for CLC-2, there is no physiological role of this interaction. Our data strongly suggest that GlialCAM stabilizes the open conformation of the common gate, providing thus mechanistic insight into the mechanism of activation of CLC-2 by GlialCAM.

SUPPORTING MATERIAL

Four figures are available at http://www.biophysj.org/biophysj/supplemental/S0006-3495(14)00785-1.

We thank A. Gradogna and S. De Stefano for supporting this work by taking care of the animal facilities, and Ilaria Zanardi for support in cell culture. We also thank F. Quartino, A. Barbin, and D. Magliozzi for expert technical assistance.

The financial support by Telethon Italy (grant GGP12008) and the Compagnia San Paolo is gratefully acknowledged. This study was supported in part by SAF 2009-07014 (R. E.) and SAF2012-31486 (R. E.), PS09/02672-ERARE to R. E., ELA Foundation 2009-017C4 and 2012-014C2B project (R. E.), 2009 SGR 719 (R. E.). R. E. is a recipient of an ICREA Academia prize.

REFERENCES

1. Moh, M. C., C. Zhang, …, S. Shen. 2005. Structural and functional analyses of a novel ig-like cell adhesion molecule, hepaCAM, in the human breast carcinoma MCF7 cells. *J. Biol. Chem.* 280:27366–27374.
2. Favre-Kontula, L., A. Rolland, …, U. Boschert. 2008. GlialCAM, an immunoglobulin-like cell adhesion molecule is expressed in glial cells of the central nervous system. *Glia.* 56:633–645.
3. López-Hernández, T., M. C. Ridder, …, M. S. van der Knaap. 2011. Mutant GlialCAM causes megalencephalic leukoencephalopathy with subcortical cysts, benign familial macrocephaly, and macrocephaly with retardation and autism. *Am. J. Hum. Genet.* 88:422–432.
4. van der Knaap, M. S., P. G. Barth, …, J. Valk. 1995. Leukoencephalopathy with swelling and a discrepantly mild clinical course in eight children. *Ann. Neurol.* 37:324–334.
5. Leegwater, P. A., B. Q. Yuan, …, M. S. van der Knaap. 2001. Mutations of MLC1 (KIAA0027), encoding a putative membrane protein, cause megalencephalic leukoencephalopathy with subcortical cysts. *Am. J. Hum. Genet.* 68:831–838.
6. Jeworutzki, E., T. López-Hernández, …, R. Estévez. 2012. GlialCAM, a protein defective in a leukodystrophy, serves as a ClC-2 Cl(-) channel auxiliary subunit. *Neuron.* 73:951–961.
7. Blanz, J., M. Schweizer, …, T. J. Jentsch. 2007. Leukoencephalopathy upon disruption of the chloride channel ClC-2. *J. Neurosci.* 27:6581–6589.
8. van der Knaap, M. S., I. Boor, and R. Estévez. 2012. Megalencephalic leukoencephalopathy with subcortical cysts: chronic white matter oedema due to a defect in brain ion and water homoeostasis. *Lancet Neurol.* 11:973–985.
9. Depienne, C., M. Bugiani, …, M. S. van der Knaap. 2013. Brain white matter oedema due to ClC-2 chloride channel deficiency: an observational analytical study. *Lancet Neurol.* 12:659–668.
10. Hoegg-Beiler, M. B., S. Sirisi, …, T. J. Jentsch. 2014. Disrupting MLC1 and GlialCAM and ClC-2 interactions in leukodystrophy entails glial chloride channel dysfunction. *Nat. Commun.* 5:3475.
11. Gradogna, A., E. Babini, …, M. Pusch. 2010. A regulatory calcium-binding site at the subunit interface of CLC-K kidney chloride channels. *J. Gen. Physiol.* 136:311–323.
12. Pusch, M., U. Ludewig, and T. J. Jentsch. 1997. Temperature dependence of fast and slow gating relaxations of ClC-0 chloride channels. *J. Gen. Physiol.* 109:105–116.
13. Gründer, S., A. Thiemann, …, T. J. Jentsch. 1992. Regions involved in the opening of CIC-2 chloride channel by voltage and cell volume. *Nature.* 360:759–762.
14. Lorenz, C., M. Pusch, and T. J. Jentsch. 1996. Heteromultimeric CLC chloride channels with novel properties. *Proc. Natl. Acad. Sci. USA.* 93:13362–13366.
15. Accardi, A., L. Ferrera, and M. Pusch. 2001. Drastic reduction of the slow gate of human muscle chloride channel (ClC-1) by mutation C277S. *J. Physiol.* 534:745–752.
16. Chen, T. Y., and C. Miller. 1996. Nonequilibrium gating and voltage dependence of the ClC-0 Cl^- channel. *J. Gen. Physiol.* 108:237–250.
17. Stauber, T., S. Weinert, and T. J. Jentsch. 2012. Cell biology and physiology of CLC chloride channels and transporters. *Compr Physiol.* 2:1701–1744.
18. Estévez, R., T. Boettger, …, T. J. Jentsch. 2001. Barttin is a Cl^- channel beta-subunit crucial for renal Cl^- reabsorption and inner ear K^+ secretion. *Nature.* 414:558–561.
19. Trichas, G., J. Begbie, and S. Srinivas. 2008. Use of the viral 2A peptide for bicistronic expression in transgenic mice. *BMC Biol.* 6:40.
20. Chen, T. Y. 1998. Extracellular zinc ion inhibits ClC-0 chloride channels by facilitating slow gating. *J. Gen. Physiol.* 112:715–726.
21. Ludewig, U., T. J. Jentsch, and M. Pusch. 1997. Inward rectification in ClC-0 chloride channels caused by mutations in several protein regions. *J. Gen. Physiol.* 110:165–171.
22. Ludewig, U., T. J. Jentsch, and M. Pusch. 1997. Analysis of a protein region involved in permeation and gating of the voltage-gated *Torpedo* chloride channel ClC-0. *J. Physiol.* 498:691–702.
23. Ludewig, U., M. Pusch, and T. J. Jentsch. 1997. Independent gating of single pores in CLC-0 chloride channels. *Biophys. J.* 73:789–797.
24. Ludewig, U., M. Pusch, and T. J. Jentsch. 1996. Two physically distinct pores in the dimeric ClC-0 chloride channel. *Nature.* 383:340–343.
25. Pusch, M., U. Ludewig, …, T. J. Jentsch. 1995. Gating of the voltage-dependent chloride channel CIC-0 by the permeant anion. *Nature.* 373:527–531.
26. Lin, Y. W., C. W. Lin, and T. Y. Chen. 1999. Elimination of the slow gating of ClC-0 chloride channel by a point mutation. *J. Gen. Physiol.* 114:1–12.
27. Accardi, A., and M. Pusch. 2003. Conformational changes in the pore of CLC-0. *J. Gen. Physiol.* 122:277–293.
28. Traverso, S., G. Zifarelli, …, M. Pusch. 2006. Proton sensing of CLC-0 mutant E166D. *J. Gen. Physiol.* 127:51–65.
29. Zifarelli, G., and M. Pusch. 2010. The role of protons in fast and slow gating of the Torpedo chloride channel ClC-0. *Eur. Biophys. J.* 39:869–875.
30. Dutzler, R., E. B. Campbell, and R. MacKinnon. 2003. Gating the selectivity filter in ClC chloride channels. *Science.* 300:108–112.
31. Estévez, R., M. Pusch, …, T. J. Jentsch. 2004. Functional and structural conservation of CBS domains from CLC chloride channels. *J. Physiol.* 557:363–378.
32. Yusef, Y. R., L. Zúñiga, …, F. V. Sepúlveda. 2006. Removal of gating in voltage-dependent ClC-2 chloride channel by point mutations affecting the pore and C-terminus CBS-2 domain. *J. Physiol.* 572:173–181.
33. Lange, P. F., L. Wartosch, …, J. C. Fuhrmann. 2006. ClC-7 requires Ostm1 as a beta-subunit to support bone resorption and lysosomal function. *Nature.* 440:220–223.
34. Leisle, L., C. F. Ludwig, …, T. Stauber. 2011. ClC-7 is a slowly voltage-gated 2Cl(-)/1H(+)-exchanger and requires Ostm1 for transport activity. *EMBO J.* 30:2140–2152.

35. Waldegger, S., N. Jeck, …, H. W. Seyberth. 2002. Barttin increases surface expression and changes current properties of ClC-K channels. *Pflugers Arch.* 444:411–418.

36. Capdevila-Nortes, X., T. López-Hernández, …, R. Estévez. 2013. Insights into MLC pathogenesis: GlialCAM is an MLC1 chaperone required for proper activation of volume-regulated anion currents. *Hum. Mol. Genet.* 22:4405–4416.

37. Traverso, S., L. Elia, and M. Pusch. 2003. Gating competence of constitutively open CLC-0 mutants revealed by the interaction with a small organic Inhibitor. *J. Gen. Physiol.* 122:295–306.

38. Miller, C., and M. M. White. 1984. Dimeric structure of single chloride channels from *Torpedo* electroplax. *Proc. Natl. Acad. Sci. USA.* 81:2772–2775.

39. Pusch, M., S. E. Jordt, …, T. J. Jentsch. 1999. Chloride dependence of hyperpolarization-activated chloride channel gates. *J. Physiol.* 515:341–353.

40. Saviane, C., F. Conti, and M. Pusch. 1999. The muscle chloride channel ClC-1 has a double-barreled appearance that is differentially affected in dominant and recessive myotonia. *J. Gen. Physiol.* 113:457–468.

41. Pusch, M., and T. J. Jentsch. 2005. Unique structure and function of chloride transporting CLC proteins. *IEEE Trans. Nanobioscience.* 4:49–57.

42. Accardi, A., and M. Pusch. 2000. Fast and slow gating relaxations in the muscle chloride channel CLC-1. *J. Gen. Physiol.* 116:433–444.

43. Duffield, M., G. Rychkov, …, M. Roberts. 2003. Involvement of helices at the dimer interface in ClC-1 common gating. *J. Gen. Physiol.* 121:149–161.

44. Niemeyer, M. I., L. P. Cid, …, F. V. Sepúlveda. 2009. Voltage-dependent and -independent titration of specific residues accounts for complex gating of a ClC chloride channel by extracellular protons. *J. Physiol.* 587:1387–1400.

45. Niemeyer, M. I., L. P. Cid, …, F. V. Sepúlveda. 2003. A conserved pore-lining glutamate as a voltage- and chloride-dependent gate in the ClC-2 chloride channel. *J. Physiol.* 553:873–879.

46. Varela, D., M. I. Niemeyer, …, F. V. Sepúlveda. 2002. Effect of an N-terminus deletion on voltage-dependent gating of the ClC-2 chloride channel. *J. Physiol.* 544:363–372.

47. Zúñiga, L., M. I. Niemeyer, …, F. V. Sepúlveda. 2004. The voltage-dependent ClC-2 chloride channel has a dual gating mechanism. *J. Physiol.* 555:671–682.

48. Garcia-Olivares, J., A. Alekov, …, C. Fahlke. 2008. Gating of human ClC-2 chloride channels and regulation by carboxy-terminal domains. *J. Physiol.* 586:5325–5336.

49. Thiemann, A., S. Gründer, …, T. J. Jentsch. 1992. A chloride channel widely expressed in epithelial and non-epithelial cells. *Nature.* 356:57–60.

50. Bennetts, B., M. L. Roberts, …, G. Y. Rychkov. 2001. Temperature dependence of human muscle ClC-1 chloride channel. *J. Physiol.* 535:83–93.

51. Fong, P., A. Rehfeldt, and T. J. Jentsch. 1998. Determinants of slow gating in ClC-0, the voltage-gated chloride channel of *Torpedo marmorata*. *Am. J. Physiol.* 274:C966–C973.

52. Maduke, M., C. Williams, and C. Miller. 1998. Formation of CLC-0 chloride channels from separated transmembrane and cytoplasmic domains. *Biochemistry.* 37:1315–1321.

53. Bykova, E. A., X. D. Zhang, …, J. Zheng. 2006. Large movement in the C terminus of CLC-0 chloride channel during slow gating. *Nat. Struct. Mol. Biol.* 13:1115–1119.

54. Ma, L., G. Y. Rychkov, …, A. H. Bretag. 2011. Movement of hClC-1 C-termini during common gating and limits on their cytoplasmic location. *Biochem. J.* 436:415–428.

55. Fischer, M., A. G. Janssen, and C. Fahlke. 2010. Barttin activates ClC-K channel function by modulating gating. *J. Am. Soc. Nephrol.* 21:1281–1289.

56. L'Hoste, S., A. Diakov, …, S. Lourdel. 2013. Characterization of the mouse ClC-K1/Barttin chloride channel. *Biochim. Biophys. Acta.* 1828:2399–2409.

57. Jordt, S. E., and T. J. Jentsch. 1997. Molecular dissection of gating in the ClC-2 chloride channel. *EMBO J.* 16:1582–1592.

58. Nehrke, K., J. Arreola, …, J. E. Melvin. 2002. Loss of hyperpolarization-activated Cl(-) current in salivary acinar cells from Clcn2 knockout mice. *J. Biol. Chem.* 277:23604–23611.

59. Gaudry, J. P., C. Arod, …, B. Antonsson. 2008. Purification of the extracellular domain of the membrane protein GlialCAM expressed in HEK and CHO cells and comparison of the glycosylation. *Protein Expr. Purif.* 58:94–102.

60. Ahmed, N., M. Ramjeesingh, …, C. E. Bear. 2000. Chloride channel activity of ClC-2 is modified by the actin cytoskeleton. *Biochem. J.* 352:789–794.